Utilizing additive manufacturing techniques to fabricate weight optimized components designed using structural optimization methods

C.J. Smith*, I. Todd* and M. Gilbert†
*Department of Materials Science and Engineering, University of Sheffield, Sheffield, S1 3JD, UK
†Department of Civil and Structural Engineering, University of Sheffield, Sheffield, S1 3JD, UK

Abstract

This paper describes a preliminary study of the application of structural optimization techniques to the design of additively manufactured components, using load testing to failure to establish true load carrying capacity. The cantilever component specimens fabricated were designed to resist a tip load and comprised one conventional benchmark design and two designs developed using layout optimization (LO) techniques. The designs were fabricated from Titanium Ti-6Al-4V and then scanned for internal defects using X-Ray Computed Tomography (XCT). All three specimens failed below the design load during testing. Several issues were identified in both the design optimization and fabrication phases of the work, contributing to the premature failure of the specimens. Various recommendations to improve the optimization phase are presented in the paper.

Introduction

Additive Manufacturing (AM) offers engineers incredible design freedoms, providing for example the opportunity to produce geometrically complex designs. This is in contrast to conventional manufacturing processes, where intrinsic limitations in the process often impose restrictions on the form of a component. Since additive manufacturing reduces these restrictions it is in principle now possible to produce much more highly optimized components. This means that designs can potentially be produced automatically using structural optimization algorithms. In this case the design problem is formulated mathematically and the ‘best’ solution is then found. What constitutes the ‘best’ solution depends on the objective of the optimization, which in the case of this paper is to minimise the weight of the component. Although minimising weight can be achieved through material optimization, as applied for example to composites and porous media (such as metal foams), this paper is concerned with weight minimisation by seeking the optimum shape or topology of the component.

Although structural optimization is a very broad research field, it is possible to categorize the methods employed as follows: (i) sizing, (ii) shape and (iii) topology optimization. Sizing and shape optimization require knowledge of the topology *a prori* as these methods can only modify the geometry, or shape, of the structure, but not the topology. Topology optimization, which is the area of focus in this paper, does not have this limitation. Whilst numerous topology optimization formulations exist, in essence they all perform the same task: for given load and support conditions the distribution of material that minimizes a specified parameter (such as mass or compliance) is sought. Depending on the formulation,

certain constraints must be enforced during the optimization process, so that the solution meets prescribed performance requirements (e.g. the yield stress is not exceeded). Most methods in the field focus on continuum idealizations of the design domain and an elastic material model. These involve discretizing the design domain with a finite element mesh and then iteratively modifying the mesh, or variables associated with elements in the mesh, until the prescribed optimization criteria has been met. Whilst these methods are very popular there remain various issues (e.g. efficiently transforming the output into a practical design).

This paper focuses instead on using the Layout Optimization (LO) procedure to generate optimized component designs. This involves the use of discrete elements interconnecting nodes positioned across the design domain and a simple rigid-plastic material model. It is suggested that this approach is likely to provide a more effective means of realising practical designs than continuum based methods.

Background on Structural Optimization

Perhaps the three most well-established continuum based methods are: (i) the Solid Isotropic Material with Penalisation (SIMP) scheme, (ii) homogenisation, and (iii) Evolutionary Structural Optimization (ESO) [1]. In SIMP the density of each element is taken as the variable in the optimization, which can vary from 0 (no material) to 1 (full material). Ideally the solution would contain only 1-0 elements and the method attempts to achieve this by penalising intermediate densities [2][3]. However intermediate densities will inevitably be present in the resulting design, necessitating a degree of subjective interpretation as to where the material boundaries lie [4]. ESO is a more intuitive optimization method that iteratively removes low stress elements (deemed to be inefficient), until a (near) fully stressed design is achieved [5]. But once an element is removed it can no longer be considered in later iterations, leading to the possibility that the design is only locally rather than globally optimal [6]. In recent years non-traditional methods such as genetic algorithms and simulated annealing have become more prevalent due to their robustness, ability to produce 1-0 solutions and simpler problem formulation [7]. However, a significant disadvantage to these methods is that they require a great deal of computing power, which limits problem size [8].

The Layout Optimization (LO) procedure discussed herein produces topologies comprising 1-D truss elements. The optimization is performed using a Linear Programming (LP) formulation that considers axial forces within the truss elements only. (If moments at the joints were to be considered then a more complicated, non-linear problem, would have to be formulated.) Although this is a significant simplification there are advantages in keeping the problem linear. Firstly, finding the global minimum is effectively guaranteed due to the convex nature of the problem. And secondly an adaptive solution scheme developed by Gilbert and Tyas, that permits very large-scale problems to be solved, can be incorporated into the optimization process [9].

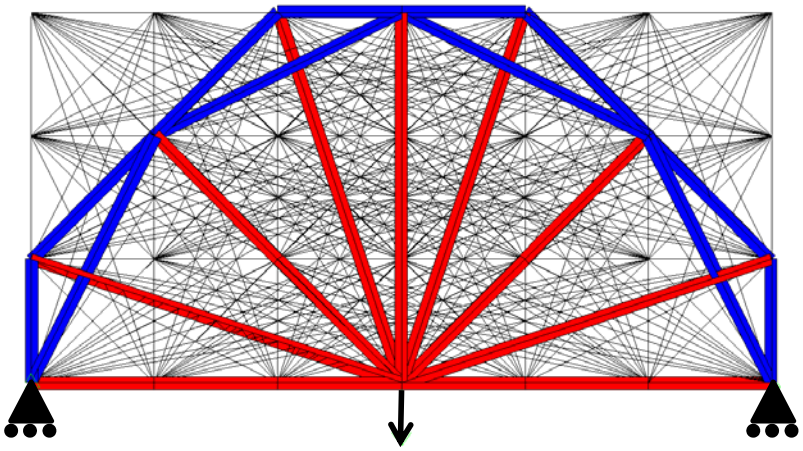

Figure 1 – Simple 2-D problem with a central point load and two pin/roller supports

The traditional LO procedure starts with a 'ground structure' consisting of a network of potential members, as shown by the black lines in

Figure 1. Loads and support conditions are then applied at the relevant nodes. Assuming a single load case and a ground structure comprising *m* members and *n* nodes, the LP formulation may be stated as follows:

$$\min \quad V = \mathbf{c}^{\mathbf{T}}\mathbf{q}$$

subject to

$$\mathbf{Bq} = \mathbf{f} \tag{1}$$

$$q_i^+, \; q_i^- \geq 0, i = 1,\ldots,m$$

Where V is the total volume of the structure, $\mathbf{q}^{\mathbf{T}} = \{q_1^+, -q_1^-, q_2^+, -q_2^-, \ldots -q_m^-\}$, $\mathbf{c}^{\mathbf{T}} = \{l_1/\sigma_1^+, -l_1/\sigma_1^-, l_2/\sigma_2^+, -l_2/\sigma_2^-, \ldots -l_m/\sigma_m^-\}$, **B** is a suitable ($2n \times 2m$) equilibrium matrix and $\mathbf{f}^{\mathbf{T}} = \{f_1^x, f_1^y, f_2^x, f_2^y, \ldots f_n^y\}$. And where l_i, q_i^+, q_i^-, σ_i^+, σ_i^- represent respectively the length and tensile and compressive member forces and stresses in member *i*. Finally, f_j^x, f_j^y are *x* and *y* direction live load components applied to node *j*. Using this formulation the linear programming problem variables are clearly the member forces, q_i^+, q_i^-.

In the case of the structure shown in

Figure 1, out of the 378 potential members in the original 'ground structure', only 18 have an area above zero at the end of the optimization process. However, if only a single load case is used then it is possible that the solution will be a mechanism (i.e. will be unstable for any load other than the design load [10]). For practical purposes it is therefore advisable to use multiple load cases to avoid this. This necessitates the introduction of 'area' variables in the formulation, which remains comparatively simple. Note that using a plastic rather than elastic formulation is advantageous when multiple load cases are involved. This is because computational difficulties can arise when attempting to use multiple load cases in elastic stress limited optimization, such as the optimality criteria method [9].

Experimental Procedure

Optimization

Next an application of the layout optimization process outlined above will be described. Three components were designed to satisfy the constraints defined in Figure 2, comprising one benchmark component and two optimized components. The problem involves a design space of 150×50×50mm with a single load of 100kN at one end and four support points at the other. A simple four bar truss design shown in Figure 3 was used as a benchmark (cantilever 1). Two optimized designs were then produced using the LO method described previously, but with differing design requirements. For both cases the design space was populated with 325 nodes equidistant to one another at a spacing of 12.5 mm. Then a ground structure with full connectivity was generated by connecting each node with every other node. However in the case of cantilever 3 a cubic lattice structure filling the entire design space was generated (shown in green in Figure 4). This was to investigate a scenario in which the whole design domain is required to be populated with a lattice structure, with in this case optimization being used to identify where the lattice structure should be reinforced.

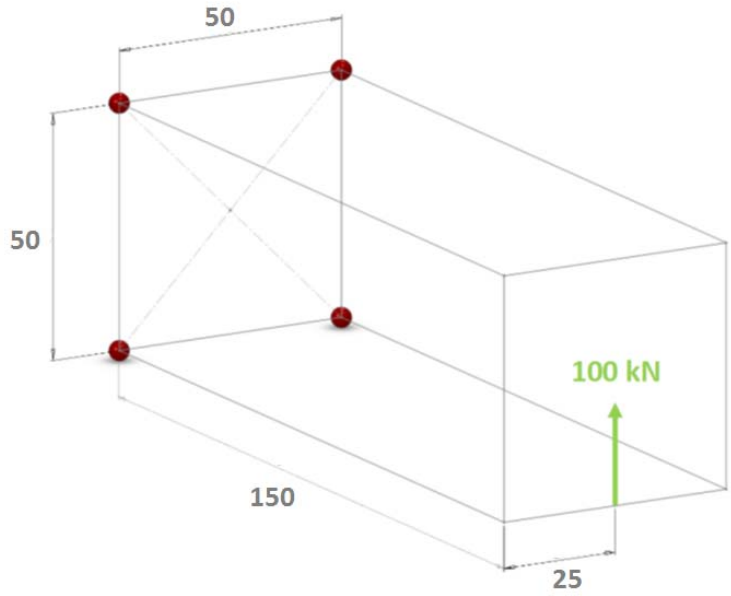

Figure 2 - Problem definition (design domain, supports and loading). Dimensions in mm

In each case several post-processing measures were performed after each optimization. The cross-sectional area of each compressive member was checked against the Euler buckling criteria (assuming a circular cross-section) as indicated in eq (2) and resized if below the critical area.

$$A_e \geq \frac{4F_e(\mathrm{KL}_e)^2}{\pi E} \tag{2}$$

Where A_e, F_e and L_e are respectively the area, limiting compressive force and length of element e. K is the column effective length factor which is set at 0.699 (fixed-free arrangement). Finally, E is the modulus of elasticity which was here taken as 113.8 GPa.

All members with a diameter below 1.5mm were then resized to this minimum value (with the exception of the background lattice elements in cantilever 3). Because minimum area and buckling constraints are considered in a post-processing phase, and not in the optimization phase, it can be argued that the result is no longer optimal. But as can be seen from Table 1, the only component that increased in mass after post-processing was cantilever 2, and then only by 1%.

Cantilever 2 was 22.7% lighter than the benchmark (cantilever 1) whereas cantilever 3 was 1.41% heavier due to the presence of the background lattice.

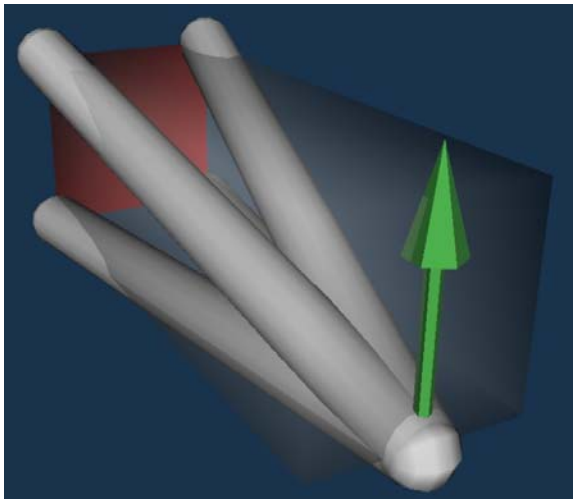

Figure 3 – Benchmark design - cantilever 1

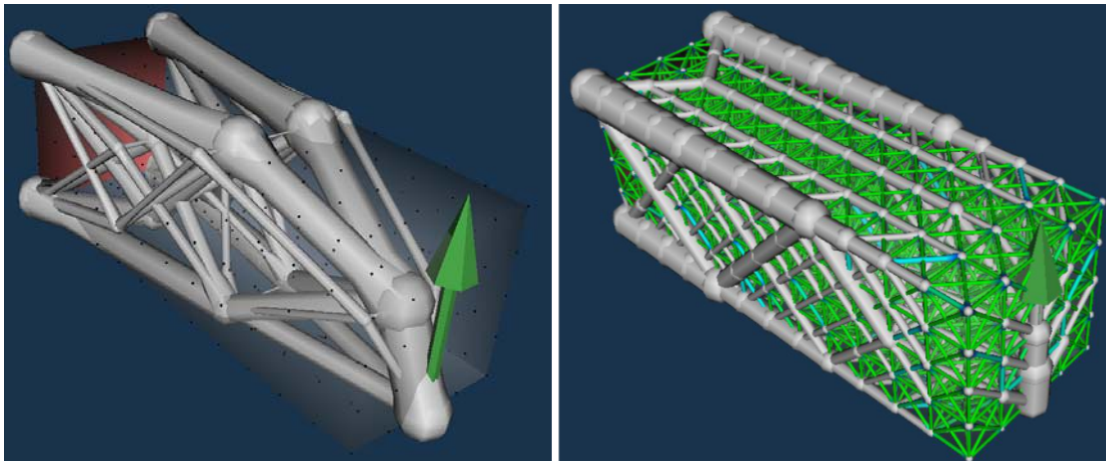

(a) **(b)**

Figure 4 – Optimized designs – (a) cantilever 2, (b) cantilever 3

Component	Volume (mm^3)	Mass (g)	Mass after post-processing (g)	Weight Reduction (%)
Cantilever 1	121875	539.9	539.9	--
Cantilever 2	93175.8	412.8	417.0	22.7
Cantilever 3	123581	547.5	547.5	-1.41

Table 1 - Mass comparison of three cantilever specimens

Fabrication

All specimens were fabricated using an Arcam S12 EBM machine. Standard Arcam process themes were used ('preheat', wafer support', 'melt' and, in the case of cantilever 3, the 'nett' theme). In addition to these, a modified process theme was used for the pin supports. The powder used was Arcam supplied gas atomised Ti-6Al-4V. Layers were deposited at a thickness of 70μm.

At the time of fabrication the machine that was originally intended to manufacture each specimen became unavailable indefinitely. The alternative route was to use another Arcam S12 EBM machine which had a smaller build envelope, only permitting builds of up to 180mm in height. As each specimen was 205mm in height a scaling factor of 0.85 was applied to the length dimension in all three Cartesian axes. The truss areas were therefore reduced by a factor of $0.85^2 = 0.7225$.

X-Ray Computed Tomography (XCT)

The EBM process is known to produce a certain degree of porosity in components made from titanium. Although this is generally more of an issue for fatigue properties it is possible that a significantly sized pore within a thin truss bar could have an influence on its strength. Before load testing an XCT analysis was performed on each optimized specimen to identify any significant defects.

The two specimens were scanned at the Henry Moseley X-Ray imaging facility at the University of Manchester, UK. Using the Nikon Metric Custom Bay a resolution of 38.9 μm was achieved for both specimens using a 1mm copper filter and a silver detector.

Load Testing

Load testing was performed using a universal testing machine in an asymmetric three point flexural bend test arrangement. Each test specimen rested on two pairs of titanium blocks at the tip and at the base. The surfaces in contact with the test specimen had grooves that were 0.5mm larger in radius than that of the circular contact points on the specimen. This offset was in place to account for the presence of a PTFE sheet between the specimen and the grooved blocks. PTFE sheet was also used between the grooved and non-grooved titanium block supports. A further grooved titanium block (with the same enlarged radius) was used as an interface between the specimen and the loading platen of the universal testing machine, again with the contact surfaces lined with PTFE sheet. All contact surfaces were polished.

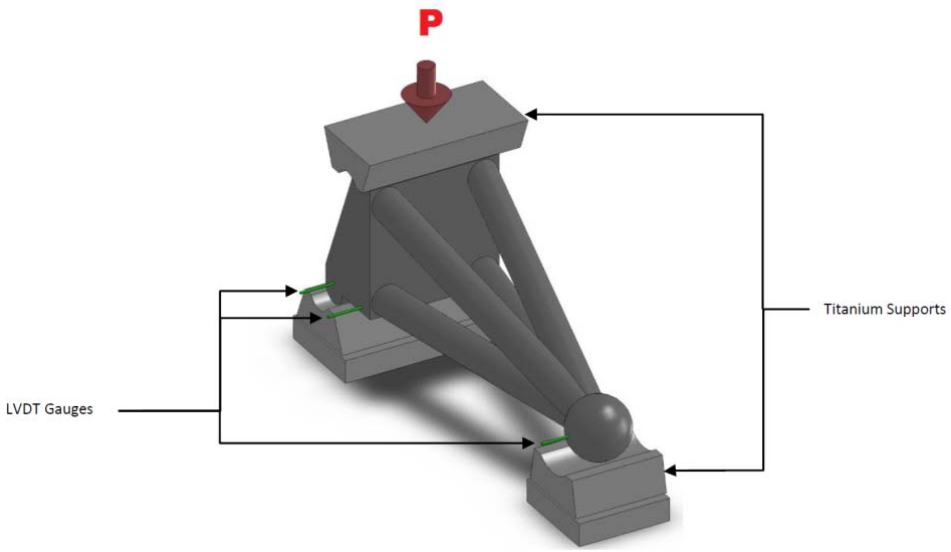

Figure 5 - Load test arrangement

To achieve an equivalent tip load of 100 kN the corresponding load applied by the testing machine would have needed to be 720 kN. However after applying the 0.85 scaling factor, the equivalent tip load reduces to 72.3 kN and the load applied by the testing machine to 610.3 kN.

Results and Discussion

XCT

Pores were identified in both cantilevers 1 and 2, as indicated in Figure 6 and Figure 7. The indicated size distribution (spherical equivalent diameter) of the pores for both specimens is shown in Figure 8. Whilst the mean equivalent diameter of the pores in cantilever 2 may be considered acceptable for static mechanical applications, this is not the case for cantilever 3, with the indicated mean equivalent pore diameter of 0.7mm being of the same order as the diameter of most truss bars (1.5mm).

Table 2 – Mean equivalent diameters of pores in cantilevers 1 and 2

	Mean Equivalent diameter (mm)	Standard Deviation ($x10^{-2}$)
Cantilever 2	0.15	4.9
Cantilever 3	0.70	47

However it was subsequently found that this was an anomalous value originating from the image reconstruction process. In this process the contrast of the image is adjusted to account for a phenomenon known as beam hardening, which occurs when low energy photons are rapidly attenuated as the beam passes through the material. But in compensating for this it is possible that the reconstructed image will contain artefacts, which are features that can be mistaken for pores or other internal defects [11]. Since the large pores always

appeared in pairs (in the same image slice), and always at the centroid of the truss members it is almost certain that they were artefacts. This was confirmed after the load tests, as no such pores were found via visual inspection.

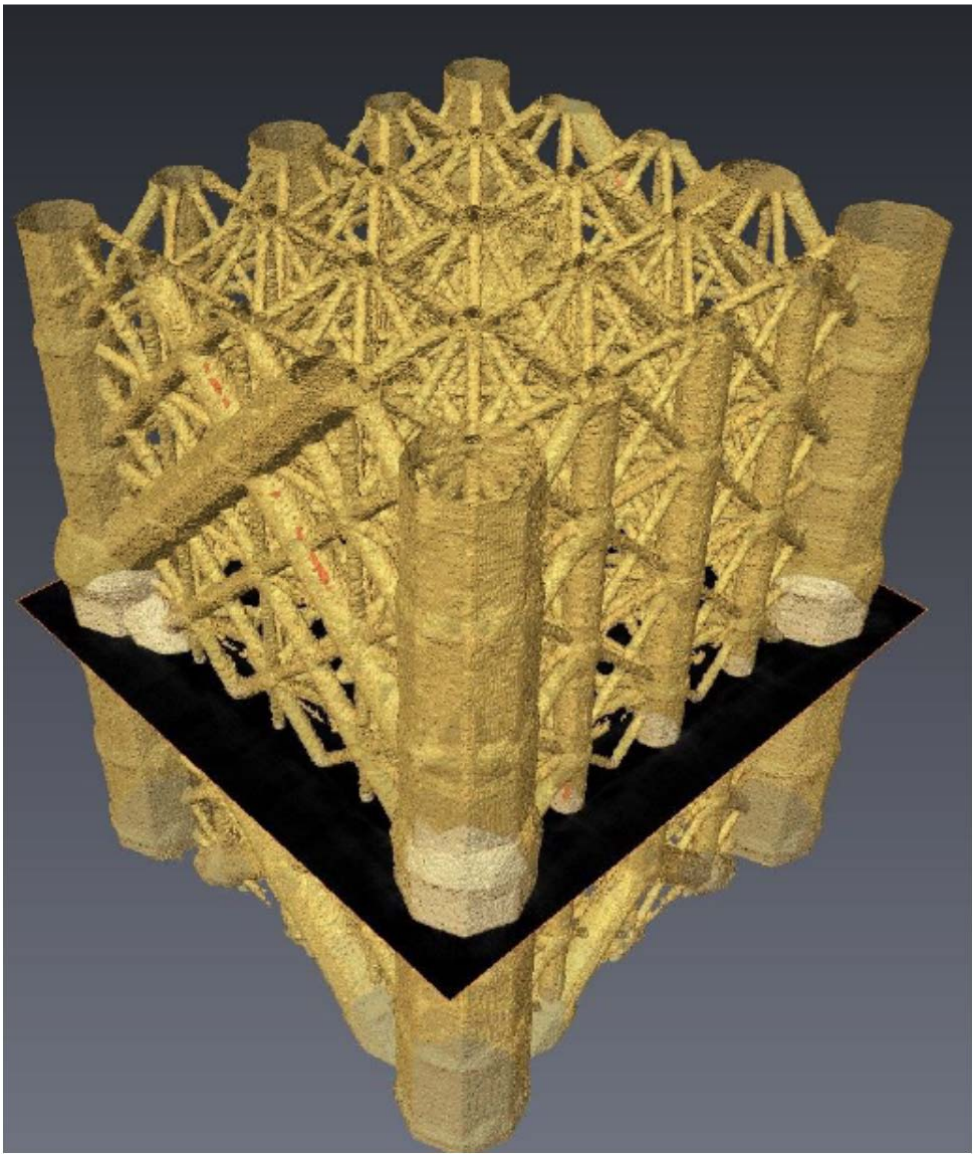

Figure 6 - Section of cantilever 3 from XCT scan. (Regions highlighted in red denote pores.)

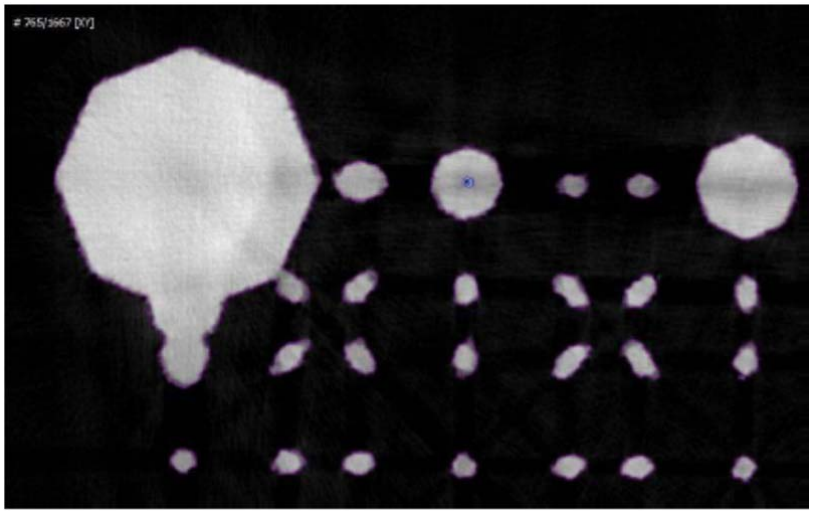

Figure 7 - Image slice showing a pore in one of the vertical members of cantilever 3

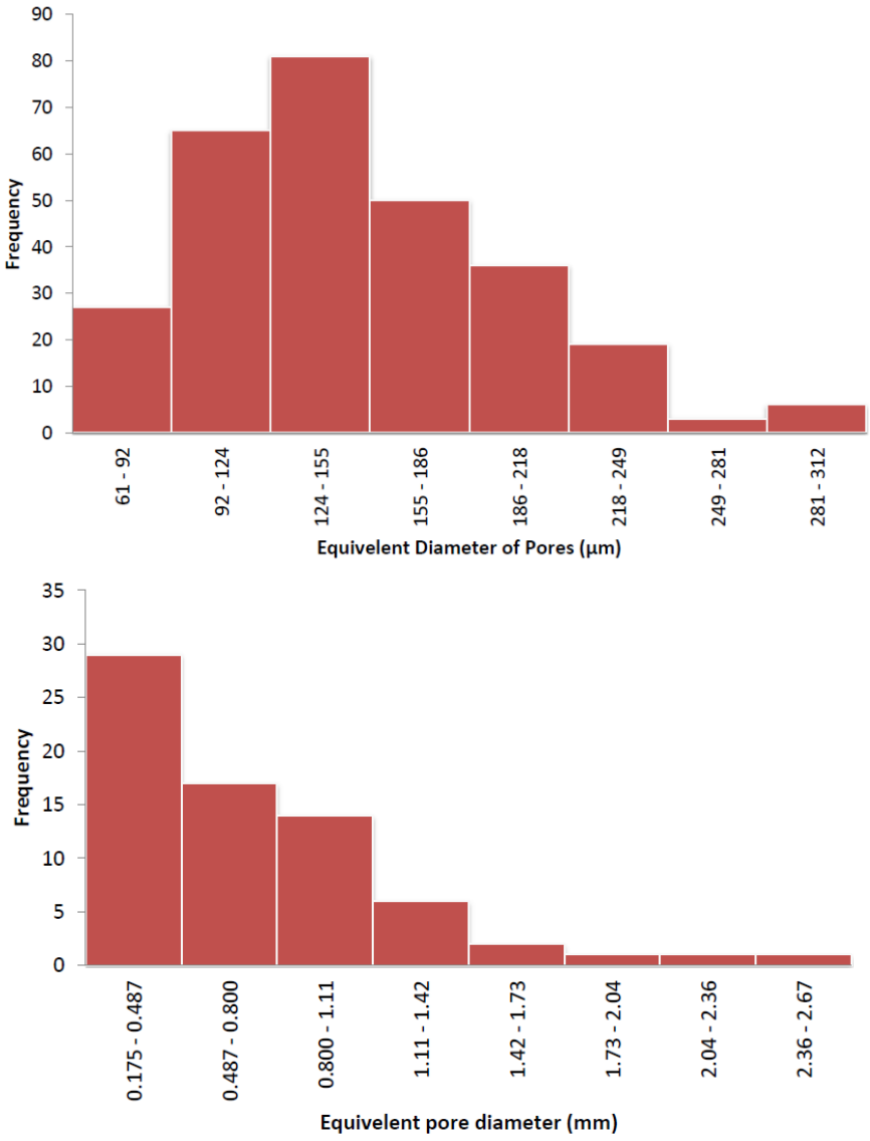

Figure 8 - Porosity size distribution for cantilever 2 (top) and cantilever 3 (bottom)

Load Testing

During load testing all three test specimens were found to fail prematurely. The load displacement curves are shown in Figure 9 with the recorded failure loads shown in

(a) Table 3. Unlike the other two specimens, cantilever 1 did not fail by fracture. Instead the top two compressive members buckled (

(b)

Figure 10). Cantilever 2 failed in two stages, starting with a failure of two cross-link members and then followed by fractures at five truss intersections. These two failures are respectively labelled (1) and (2) in Figure 12. Cantilever 3 suffered a very sudden failure at the interface between the specimen and the base structures; inspection of video captured during the test suggested that the specimen failed in shear.

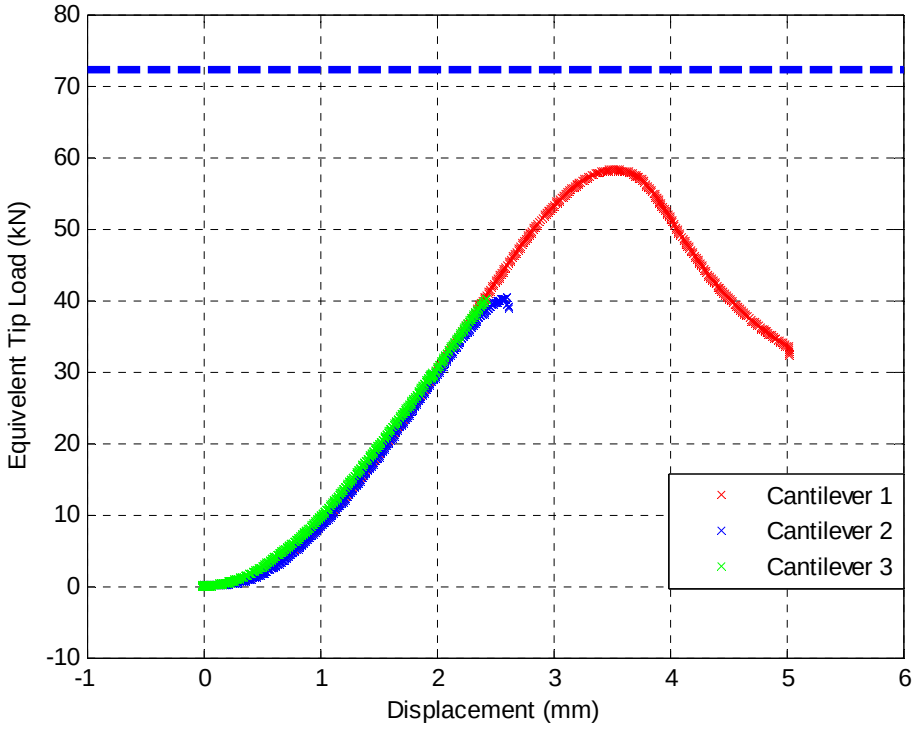

Figure 9 - Load-Displacment curves for all three cantilever speciments. Blue dashed line denotes design load

Table 3 – Load at failure for each cantilever specimen

Component	Ultimate Tip Load (kN)
Cantilever 1	58.3
Cantilever 2	40.3
Cantilever 3	40.2

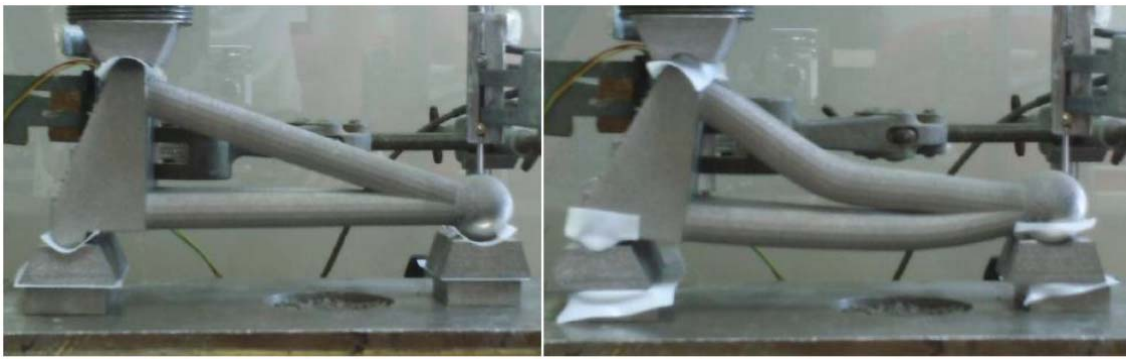

(b) **(b)**

Figure 10 - Cantilever 1 (a) at the start and (b) at the end of the test

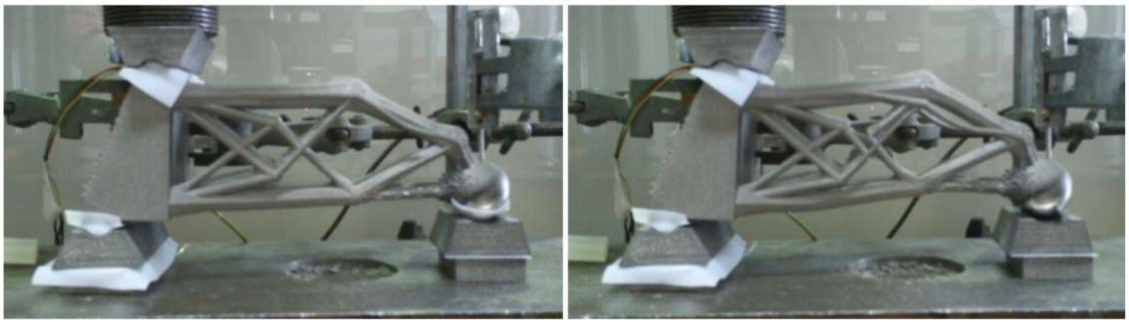

(a) **(b)**

Figure 11 - Cantilever 2 (a) at the start and (b) at the end of the test

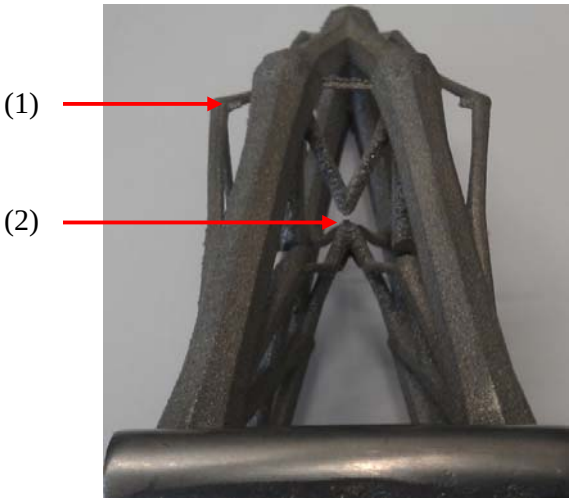

Figure 12 - Failure of cantilever 2

Recalling that the specimens were fabricated at 85% of their originally intended size, it might be supposed that the load bearing capacity would be 72.3% of the original design value ($72.3\% = 0.85^2 \times 100\%$), considering area reduction alone. But additional factors make this simplistic assumption incorrect. Firstly, during the post-processing phase all members were checked to see if they were susceptible to buckling, and that they had diameters above the

minimum threshold of 1.5 mm. Any members in violation of one or other of these criteria had their cross-sectional area adjusted. However these measures were not performed *after* scaling, and as a consequence there were members present in cantilever 2 that violated both criteria.

Furthermore, in the case of cantilever 2 there were two other significant issues that contributed to the premature failure. Firstly, at the locations of the first failure (the cross-links labelled (1) in Figure 12) there were several collinear overlapping members in the solution. The sum of the areas of the three overlapping members at the failed cross-link was 0.622 mm^2. But the actual cross-link area was just 0.367 mm^2, 58% of what it should have been. i.e. a failure to identify overlapping members in the post-processing phase led to a unintentional stress concentration at each of these locations. Secondly, at five cross-over locations (labelled (2) in Figure 12) there were also stress concentrations. Extra material was added at joints to avoid stress concentrations but the simple post-processing routine employed only performed this measure at nodes, omitting to add material at the five cross-overs indicated in Figure 13.

In the case of cantilever 3, this suffered a very abrupt failure at the interface between the specimen and the base structure. Inspection of video footage taken during the test suggested that the specimen failed in shear. However, the fracture surfaces shown in Figure 14 show a 'cup and cone' failure on two of the four largest members at the base. As these members would have been in tension it is possible that the bending moment capacity of the specimen had been exceeded during the test. However, a simple shear force and bending analysis predicted that the Von Mises stress at failure was below the yield stress of Ti-6Al-4V. (Though note that this analysis did not take into account the deformed geometry of the structure at failure, and it is possible that the deformed shape of the structure could have markedly altered the distribution of internal forces.)

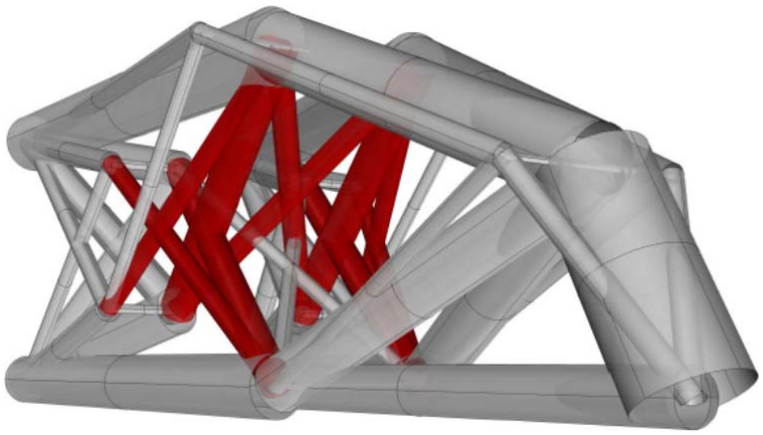

Figure 13 - Truss volumes of cantilever 2 (members failing after the first two cross-links are indicated in red)

Figure 14 - Cantilever 3 post-test with fracture surfaces shown

Concluding remarks

- Layout optimization (LO) has been used to identify structurally optimized forms for a simple additively manufactured cantilever component. The LO technique appears to be a promising alternative to more widely used continuum topology optimization methods for this application.
- Two very different optimized designs were developed using LO, illustrating the ability of this method to take account of specific user requirements.
- Three additively manufactured specimens were load tested, but all failed prematurely (the benchmark component, cantilever 1, and the two optimized components, cantilever 2 and 3).
- X-Ray Computed Tomography (XCT) revealed that pores were present in both the specimens which were scanned (cantilevers 2 and 3) but the size of the pores would have likely had negligible influence on the static mechanical properties of the specimens. (Larger pores were initially identified in cantilever 3, but these were determined to be anomalies originating from the image reconstruction process.)
- For logistical reasons the components had to be scaled down geometrically shortly before fabrication, but this meant that elements in cantilever 2 became susceptible to buckling and/or fell below the 1.5mm minimum diameter design threshold.
- The presence of overlapping and/or intersecting members which were not dealt with in the post-processing phase (by introducing additional material) have been identified as the main cause of the premature failure of cantilever 2. New post-processing routines have been introduced to rectify this.
- The classical Euler buckling criteria used is likely to over-simplify the behaviour of the truss elements, and its use is being reviewed. The buckling characteristics of Ti-6Al-4V specimens produced using the EBM process will also be investigated experimentally.
- New re-designed specimens will shortly be produced to address the issues identified in this preliminary study.

References

[1] Bureerat S, Limtragool J. Finite Elements in Analysis and Design 2008;44:738.

[2] Bendsøe MP. Structural and Multidisciplinary Optimization 1989;202:193.

[3] Eschenauer H a, Olhoff N. Applied Mechanics Reviews 2001;54:331.

[4] Lu K-J, Kota S. Journal of Mechanical Design 2006;128:1080.

[5] Xie Y. Computers & Structures 1993;49:885.

[6] Rozvany G. Structural and Multidisciplinary Optimization 2001;21:109.

[7] Lagaros ND, Papadrakakis M, Kokossalakis G. Computers & Structures 2002;80:571.

[8] Sigmund O. Structural and Multidisciplinary Optimization 2011;43:589.

[9] Gilbert M, Tyas A. Engineering Computations 2003;20:1044.

[10] Bendsoe MP, Sigmund O. Topology Optimization: Theory, Methods and Applications. Springer; 2003.

[11] Kruth JP, Bartscher M, Carmignato S, Schmitt R, De Chiffre L, Weckenmann a. CIRP Annals - Manufacturing Technology 2011;60:821.